Dalton Transactions

Accepted Manuscript

This is an *Accepted Manuscript*, which has been through the RSC Publishing peer review process and has been accepted for publication.

Accepted Manuscripts are published online shortly after acceptance, which is prior to technical editing, formatting and proof reading. This free service from RSC Publishing allows authors to make their results available to the community, in citable form, before publication of the edited article. This *Accepted Manuscript* will be replaced by the edited and formatted *Advance Article* as soon as this is available.

To cite this manuscript please use its permanent Digital Object Identifier (DOI®), which is identical for all formats of publication.

More information about *Accepted Manuscripts* can be found in the **Information for Authors**.

Please note that technical editing may introduce minor changes to the text and/or graphics contained in the manuscript submitted by the author(s) which may alter content, and that the standard **Terms & Conditions** and the **ethical guidelines** that apply to the journal are still applicable. In no event shall the RSC be held responsible for any errors or omissions in these *Accepted Manuscript* manuscripts or any consequences arising from the use of any information contained in them.

Graphical Abstract

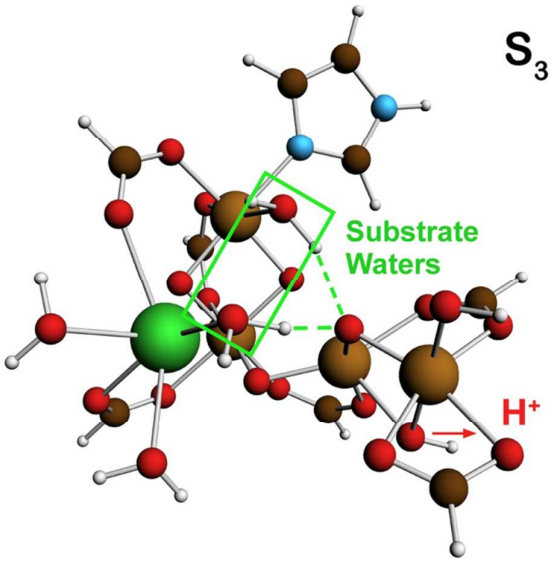

Thermodynamic principles for the operation of the water oxidising Mn_4/Ca cluster within Photosystem II are examined in the light of the known redox chemistry of hydrated Mn-oxo compounds.

Why Nature chose Mn for the Water Oxidase in Photosystem II

Ron J. Pace *, Rob Stranger and Simon Petrie
Research School of Chemistry, College of Physical and Mathematical Sciences,
Australian National University
Canberra ACT Australia

Abstract

Nature performs a vital but uniquely energetic reaction within Photosystem II (PS II), resulting in the oxidation of two water molecules to yield O_2 and bio-energetic electrons, as reducing equivalents. Almost all life on earth ultimately depends on this chemistry, which occurs with remarkable efficiency within a tetramanganese and calcium cluster in the photosystem. The thermodynamic constraints for the operation of this water oxidising Mn_4/Ca cluster within PS II are discussed. These are then examined in the light of the known redox chemistry of hydrated Mn-oxo systems and relevant model compounds. It is shown that the latest high resolution crystal structure of cyanobacterial PS II suggests an organization of the tetra-nuclear Mn cluster that naturally accommodates the stringent requirements for successive redox potential constancy with increasing total oxidation state, which the enzyme function imposes. This involves one region of the Mn_4/Ca cluster being dominantly involved with substrate water binding, while a separate, single Mn is principally responsible for the redox accumulation function. Recent high level computational chemical investigations by the authors strongly support this, with a computed pattern of Mn oxidation states throughout the catalytic cycle being completely consistent with this interpretation. Strategies to design synthetic, bio-mimetic constructs utilising this approach for efficient electrolytic generation of hydrogen fuel within Artificial Photosynthesis are briefly discussed.

*Correspondence:
Ron J. Pace: Ron.Pace@anu.edu.au

Introduction

The mechanism of water oxidation, to yield molecular oxygen and the components of hydrogen (protons and electrons), has become a focus of intense scientific inquiry in recent years and received prominent treatment in this journal [1,2]. This interest is motivated by the desire to understand the water splitting process in natural photosynthesis, but also as a possible 'bio-mimetic' model for employment within Artificial Photosynthesis (AP), which is currently a program motivating a broad range of chemical-biophysical and materials science research. AP is a generic term, embracing a range of novel technologies for non-polluting electricity generation, fuel production and carbon sequestration, using solar energy. As the name implies, the inspiration is drawn from natural photosynthetic systems, which developed in organisms that were amongst the earliest known to exist on earth [3]. The natural systems are thus the product of an extremely long (> 2.5 billion years) process of evolutionary refinement.

The broader aim of AP is to technologically reproduce the components of natural photosynthesis on a large scale, for efficient solar energy conversion. This offers the prospect of economical photovoltaic electricity generation and food production requiring negligible water usage compared to conventional agriculture [4]. However, in the near term, the most feasible goal is renewable, economically competitive electrolytic or photolytic H_2 generation from convenient water sources, such as seawater. To achieve this requires a suitable 'super catalyst' for the anodic, water oxidising reaction, which is rate limiting in all conventional electrolytic systems generating H_2. In fact nature has solved this problem, within photosynthesis, almost to the absolute limit of thermodynamic efficiency.

In all oxygenic photosynthetic organisms (plants, algae, cyanobacteria etc.), the photo-excited electrons which enable all subsequent biochemical processes (notably CO_2 fixation) come from water, and this oxidation of water to molecular oxygen and protons is the ultimate source of virtually all bio-energetic electrons utilised by living creatures. The process occurs within the oxygen evolving complex (OEC) located in Photosystem-II, a large multi-subunit membrane bound protein complex. The OEC comprises an oxo bridged Mn_4/Ca cluster, with associated co-factors, notably a redox active tyrosine, Y_z [3]. All oxygenic photosynthetic organisms share a common set of 'core' membrane proteins in PS II. The evidence is very strong that the local structure and mechanism of the water splitting metal cluster within the OEC is the same in all these organisms and appears to be essentially unaltered over ~ 2 billion years at least. While at present only PS II complexes from thermophilic bacteria have been crystallised to permit X-ray diffraction study to

atomic resolution [5], there is a vast body of spectroscopic and biochemical data attesting to the fundamental uniformity of the OEC throughout nature [6]. In particular, Mn plays a critical role in the chemistry of the OEC, no other metal may functionally replace it. The Ca ion is also quite special, but may be functionally replaced by at least one other element, Sr [7]. Here we examine those properties of Mn which appear to make it uniquely suited to operate in a highly efficient water oxidase catalyst, both from a thermodynamic and kinetic standpoint. It is useful first however to briefly survey where Mn is found in natural enzymes and where it may functionally replace, or be substituted by, other metals.

Mn Enzymes.

Enzymes containing Mn ions in their catalytic regions may be broadly divided into two classes, non redox active and redox active. In both cases the metal ion is often present in bi-nuclear (occasionally higher nuclearity) sites, with bridging of the ions by solvent, hydroxo, oxo or carboxylato groups [8].

Non Redox Active: The non redox active enzymes are principally hydrolases, which catalyse the hydrolysis of peptide, ester, phosphate-ester or related (e.g. C-N in arginase) bonds. In addition to Mn (exclusively as Mn^{II}) , other generally divalent ions (Zn^{2+}, Ni^{2+}, Fe^{2+}/Fe^{3+}, Mg^{2+}) are found as homo or mixed pairs in the catalytic sites of these enzymes. Often Mn^{II} may functionally substitute for one of the other ions which constitute the native metal species. As noted by Dismukes [8], this happens because of similarities in ionic radius, Lewis acidities and pK_a of ligated water ions – the specific redox properties of the ions are largely irrelevant. Comprehensive reviews are given in [8, 9] and this class will not be considered further here.

Redox Active: This class includes superoxide dismutases, catalases and the water oxidase. The enzymes are all involved with catalysing interconversion between stable/reactive oxy-species spanning the transition between water and molecular oxygen. The various pathways are summarised in Fig. 1a.

Superoxide Dismutases (SOD): These enzymes catalyse the reactions [10];

$$SOD[M^{(n+1)+}] + O_2^- \rightarrow SOD[M^{n+}] + O_2 \quad 1)$$

$$SOD[M^{n+}] + O_2^- \rightarrow SOD[M^{(n+1)+}] + H_2O_2 \quad 2)$$

where the metal, M may be Cu (n=1) , Mn (n=2) , Fe (n=2) , Ni (n=2). In these reactions, the substrate oxidative (enzyme reductive) step, occurring within reaction 1), is actually *exothermic,* relative to the NHE (Fig.1). Thus a variety of metals, in modest oxidation states, can operate in the

active site which contains only one redox active ion undergoing one electron steps (the Cu enzyme contains a bi-nuclear, Cu/Zn^{2+} site). The reverse step 2), in which the metal is re-oxidised is also (highly) exothermic relative to NHE, so the overall process proceeds with strong driving force. For the Mn enzyme, as crystallized, the metal ligation in the active site consists of three separate Histidine nitrogens, a carboxylate and one OH(H) (substrate site) [11] (Fig. 1b). The ligand N/O ratio, the significance of which we will return to below, is ~ 1.5.

Catalases (Cat): These catalyse the concerted two electron reactions [8, 12];

$$Cat[+2] + H_2O_2 \rightarrow Cat[0] + 2H^+ + O_2 \qquad 3)$$

$$Cat[0] + H_2O_2 + 2H^+ \rightarrow Cat[+2] + 2H_2O \qquad 4)$$

Catalases are widely found in nature, in bacteria, plants and air breathing animals, i.e. virtually all organisms exposed to oxygen. Only two metals serve as redox active species in the functional sites of these enzymes, Fe and Mn. The two metals operate in very different ways. In the Fe (also called heme) catalases the Fe is contained in a heme centre and both the central Fe and the porphyrin ring undergo single electron oxidation/reduction, forming the $[Por^{+}\text{-}Fe^{IV}=O]$ and $[Por\text{-}Fe^{III}]$ species, respectively. This chemistry is quite unlike that which we know now occurs in Mn catalases and is likely in the OEC, but resembles somewhat that occurring in Mn porphyrin Jacobsen catalysts and related systems [13a,b], which we return to briefly below.[†] An extensive recent review of catalases, particularly heme catalases, is found in [12] and again we leave this enzyme class to the interested reader to pursue.

The di Mn catalases, found so far only in bacteria, are much closer to the OEC centre in general structure and likely mode of action, but although being simpler they evolved much later [12]. The catalytic site contains a (hydr)oxo, carboxylato bridged pair of Mn ions which are magnetically coupled [8,14]. Each Mn ion is terminally ligated equatorially by one Histidine nitrogen, one carboxylate oxygen and two oxo groups (Fig. 1). The overall N/O ligation ratio for Mn is ~ 0.2. For these enzymes,

$$Cat[+2] = Cat[(Mn^{3+})_2] \text{ and } Cat[0] = Cat[(Mn^{2+})_2]$$

From Fig. 1 we see that the two electron substrate oxidative (enzyme reductive) step, within reaction 3), is now significantly *endothermic*, relative to NHE, but the reverse reaction, within 4) is sufficiently exothermic that the overall dis-proportionation is thermodynamically favoured.

[†] It is a mater of historical interest that Melvin Calvin and Lord George Porter, both Nobel Laureates in chemistry, for a time suspected that the OEC water oxidase reaction involved Mn heme based chemistry and sought to mimic this with model systems involving Mn porphyrins and related species (e.g. see *New Scientist*, Vol 88, Oct 1980)

However, now that a significant multi-electron oxidation of an oxy-hydroxy substrate species is required, nature chooses only Mn to perform this function in a purely metal centred fashion. The ligand environment comprises mainly oxo, carboxylato groups and the Mn ions cycle between the II and III oxidation states. Interestingly, when the enzyme site is raised to the Mn III-IV oxidation level ('super-oxidised') by strong exogenous oxidants, it becomes inactive, but this form is an extensively used model for spectroscopic study [8,15]. The inactivation appears to be related to the loss of solvent/substrate accessible axial Jahn-Teller site(s) on Mn^{III}, where terminal binding of peroxide occurs during the substrate oxidative step, 3) [8,14] (Fig. 1c). This may have relevance for the mechanism of water oxidation in the OEC (See Mn Chemistry section below).

PS II Water Oxidase (OEC): This centre catalyses the reaction;

$$OEC[+4] + 2H_2O \rightarrow OEC[0] + 4H^+ + O_2 \qquad 5)$$

We discuss the reaction in detail below. From Fig. 1a, the substrate oxidative step within 5) is extremely endothermic relative to NHE. Now *only* Mn is found as the redox active metal in the PS II active site, despite this enzyme having evolved several billion years ago in the early Earth and having been subject to extreme evolutionary pressure.

Water Oxidation in PS II.

The water oxidation process involves three distinct steps, each operating at an efficiency near the theoretical limit and unmatched by any related synthetic system (see Fig. 2):

(i) Trapping of light energy by chlorophyll pigments and rapid energy transfer to the reaction centre (P680), resulting in its oxidation to $P680^+$.

(ii) Rapid electron donation to $P680^+$, through an oxidisable protein side chain intermediate (Tyrosine 161,Y_Z, on the D1 peptide), which stabilises the charge separation in PS II.

(iii) Oxidation of water to molecular oxygen within the OEC. This is the most energetically demanding reaction performed by nature, requiring a redox potential per electron of ~ 0.9 V (at pH ~ 6). The redox potential developed in $P680^+$ is in excess of 1.3 V, however the Y_Z intermediate has an operating potential of only 1.0-1.1 V, barely above the thermodynamic limit for OEC operation [16].

The OEC Mn/Ca cluster is thus the most efficient anodic 'electrolysis' system known. It operates under mild conditions of temperature, pH, electrolyte background etc., with a maximum turnover rate ~ 10^3/sec and effective over-voltage of at most ~ 0.1 V. It performs the reaction:

$$2H_2O \rightarrow 4H^+ + O_2 + 4e^- \qquad 6)$$

which proceeds through five intermediates consisting of four meta-stable states, labelled S_0, S_1, S_2 and S_3, and one short-lived 'final' state, S_4, where the subscript refers to the number of stored oxidising equivalents in the catalytic center. Water remains exchangeable with this site up to S_3, [17] and the final oxidation of two water molecules to di-oxygen occurs in a concerted, four electron step [6]. It is now generally held that the S states correspond to progressively increasing mean oxidation levels of the Mn ions, at least up to S_3. [18]. The sequence, with the accepted pattern of proton loss, is indicated in Fig. 3, although this proton sequence is 'idealised' and often more complex (fractional on some steps) in practice [19]. Internal release from the Mn cluster may not be rigorously in phase with release to solvent (where detection occurs).

Much detail of the Mn_4/Ca catalytic site has now been revealed by a recent crystal structure of cyanobacterial PS II to atomic resolution (1.9 Å) by Umena et al. [5], building upon earlier structures at lower resolution (2.9, 3.0 Å) [20,21]. These structures should correspond to the 'dark stable' S_1 state, although questions concerning radiation induced Mn reduction during the XRD data collection process remain [22].

The 1.9 Å structure allows a full experimental definition of the ligand environment of each metal in the OEC cluster, at least for a presumed formal S_1 state. Although the protonation state of individually resolved O atoms in not revealed, the structure is closely consistent with recent computational models of the cluster [23], derived from the protein derived ligation pattern revealed earlier by the 3.0, 2.9 Å structures. Notable is the presence of several water/hydroxide/oxo molecules binding to the fourth (so called 'dangler') Mn, which has only two protein supplied (carboxylate) ligands. The necessity for such extra O moieties had been consistently inferred from computational modelling of the site by several groups [24-27].

Fig 4 shows a comparison of the immediate OEC region from the 1.9 Å structure and our recent computational modelling of the Mn_4/Ca cluster and ligands (truncated to ligating functional groups, as in [24]). Mn numbering is according to our previous convention [24]. The model cluster is maximally 'hydrated' in that all potential direct water/hydroxide binding sites on the metals are saturated. The mean cluster oxidation state is 3.0, with a [III,IV,III,II] configuration for Mn(1)…Mn(4), and this reproduces the close metal-metal distances well resolved in EXAFS ([23] and see Fig. 6 below), but these are slightly shorter generally than the equivalent distances seen in the 1.9 Å structure. The structure and redox configuration defined computationally, we believe to be that most consistent with the photosystem in PS II samples undergoing functional turnover

[24c,24d]. However, others (e.g. [25-27]) propose a higher mean oxidation level for S_1 (3.5) and the matter is presently in contention [23]. Nonetheless, much of the discussion here does not hinge critically on this difference.

It has long been realised, from XANES and photo-assembly measurements, that the Mn in the functional OEC site have oxidation levels significantly above Mn^{II}. [28,29]. Further, the S_0 and S_2 states have odd numbers of unpaired electrons in the exchange coupled cluster, with net spin ½ ground states arising from a predominantly anti-ferromagnetic coupling of the Mn ions. They exhibit Mn hyperfine structured signals in EPR at low temperatures ('multilines'). This then dictates that the formal oxidation state in S_1 is Mn^{III}_4 or $Mn^{III}_2Mn^{IV}_2$, or combinations equivalent to these. (as alluded to above). The mean oxidation levels in the other S states are then determined by adding or removing electrons. We have labelled the above two possibilities the ‘low’ and ‘high’ oxidation state paradigms, respectively [24d]. At present, the high oxidation state assignment is generally favoured, based principally on empirical interpretation of Mn X-ray absorption spectroscopies applied to PS II in the S_1 state and S states generated by single turnover flash advance [18,28]. However, we have recently shown, using a new Time Dependent DFT (TDDFT) approach, that the results from the most extensively used X-ray absorption technique, Mn K edge analysis, are consistent with the low oxidation state paradigm [30], when metal ligand environment effects are computationally accounted for.

The fact that available structural and other data on the Mn cluster can be accommodated computationally within a low oxidation state model, as well as high, particularly for the most studied S_1 intermediate, is significant when considering possibilities for the water splitting mechanism which operates within the site. To date all such detailed proposals, arising mainly from computational chemistry [23,25,26], have assumed the high oxidation state paradigm and require one or both substrate water molecules to undergo progressive deprotonation throughout the S cycle. It is completely unclear however that this is consistent with the known pattern of substrate water exchange kinetics [17], which we examine further below.

Water Oxidation and Mn Chemistry.

Water oxidation in PS II occurs intimately within a local protein environment composed almost entirely of chemical species formed from hydrogens bonded to first row atoms (C,N,O). These groups generally require similar energies for electron removal to that for water itself. The water splitting process could therefore be likened to ‘setting a fire in a wicker basket, without burning the

basket'. There are two features of the OEC which then seem to us particularly relevant regarding its possible chemical mechanism.

1) Although the oxidised reaction centre, $P680^+$, has a redox potential of ~ 1.3-1.4 V, this is immediately 'detuned' to 1.0 -1.1 V on passage through Y_z, before communicating directly with the Mn cluster in the OEC, which must operate at a level close to 0.9 V.
2) The ligands directly bound to the Mn/Ca in the OEC are almost exclusively oxygens, from hydroxy species, oxo bridges and carboxylate protein side chains. There is only a single N ligand (out of ~ 21) from the His 332 imidazole side chain. This is the lowest known N/O ligation ratio for Mn in a protein, when the Mn oxidation states exceed II.

Examination of Fig. 1a shows that the immediate 'detuning' of the redox potential by Y_z serves to protect the 'basket', by essentially excluding the possibility of forming dangerous, reactive intermediate species like H_2O_2 or O_2^- (or even $OH^\bullet$), but at the cost of enforcing a concerted, 4 electron process for the water oxidation chemistry, which must operate in an almost 'activationless' manner (i.e. low overvoltage). Further, there is currently a large body of chemical experience with synthetic polynuclear Mn clusters of high (III, IV) formal redox level (e.g. see [2,32]). Mostly, however, these have significant, often dominant levels of N ligation (N/O ~ 2), along with oxo bridging. The N ligation provides covalent donation to Mn in high oxidation levels (IV,V), facilitating synthesis. By contrast, the predominantly O ligation in the OEC is notable because nature had the option to choose otherwise. Certainly N ligation to Mn, using histidine, imidazoles or even heme or chlorin macrocycles (as in Jacobsen catalysts [13a]) would have been easily possible in the photosystem protein matrix (see Mn Enzymes discussion above). Indeed, it has recently been demonstrated [13b] that a 'double Jacobsen' like system, involving linked near co-facial Mn porphyrin moieties, can act as a water oxidation catalyst. Here the two Mn ions operate between redox levels III and V, as a pair of two electron centres to activate O-O bond formation between two axial manganyl oxygens (derived from water). However, it is known from time resolved XANES measurements [18b] that Mn^V does not form in the OEC catalytic cycle, even in the transient S_4 state. Thus, the high oxygen ligation level must be important, functionally and is presumably related to the mean Mn oxidation levels operating in the OEC. Because oxygen, either oxo or carboxylate derived, is a significantly harder ligand than nitrogen, it is less electron donating and less able to compensate the formal charge on the ligated metal ion. Mn in an oxygen ligand environment will then generally experience a higher redox potential, for the same formal oxidation states, than with nitrogen ligation. The inference from this structural feature alone is that the Mn oxidation levels are likely to be at the *lower*, rather than *higher* end of the above two ranges of

oxidation state possibilities, if this is still consistent with the thermodynamic requirements for water oxidation.

Over the last decade synthetic, self assembled inorganic catalysts, based on Mn or Co, exhibiting efficient water electrolytic (or electro-photocatalytic) function have been developed [33]. Fig. 5A illustrates some examples. The catalysts have oxygen-bridged polynuclear, extended structures, resembling in some cases known mineral forms. We have recently [34] surveyed these and noted the similarities within their repeating units of motifs strongly resembling the compact oxo bridged core of the Mn ions in the OEC. At present it is not known which precise components of these structures actually bind water molecules and execute catalytic function. However, an interesting general reaction pathway is suggested from the known chemistry of Mn and Co, which we return to in more detail at the end of this section.

Prior to these developments, an extensive body of research had occurred (during the previous two decades) on the use of deposited hydrated metal oxide surfaces for the anodic component of electrolytic cells (e.g. see [35]). The most promising systems included oxides of the abundant transition metals from the 1st row, as well as Ru. Although detailed molecular, structural elucidation of these systems is yet to occur, important bulk physical characterisations were obtained - notably accurate mid point potentials for successive redox changes of the metals in the hydrated oxide matrices. Some relevant data are given in Table 1. What is striking about these potentials is that, despite uncertainties of oxy-hydroxides being reasonable but not exact models for the OEC etc., *ONLY* the Mn values are consistently poised, from oxidation level II to IV, to fit *precisely* into the narrow gap of redox potentials required for OEC function. To our knowledge, Mn is unique in the periodic table in this regard.

Table 1 **One/two-electron redox potentials for selected Transition Metal bulk Oxy-Hydroxides**

E^0 Reduction Potentials (V vs NHE)

Couple [a]	**Fe**	**Co**	**Mn**	**Ru**
III / II	0.27	0.87	1.0	0.24[b]
IV / III	>1.0	1.48	1.01	0.9
IV / II	-	1.18	0.9	0.0
V / IV				1.15

a) From ref [35] and references therein; b) (aq.) Ru^{3+}/Ru^{2}

The basis of the 'constant potential' effect is presumably the ability of Mn centers in the hydrated oxide environment to compensate for charge increase by release of protons from probably terminally bound water/hydroxl groups, to maintain a near invariant redox potential of the ions with increasing formal oxidation state. Some such compensation effect would of course be generally expected to occur with hydrated cations undergoing successive oxidation, but for Mn the compensation can apparently be near 'perfect'. For Co it is 'good' and likely contributes to the success of the system discovered recently by Nocera et al. [33a] (see also below). The robustness of Mn redox properties in this regard is further demonstrated by comparison of the progressive oxidation behaviours of two broadly similar Mn oxo/alkoxo bridged binuclear complexes shown in Table 2 and Scheme 1. One possesses a terminal, deprotonatable H_2O group ligated to a Mn, while the other does not.

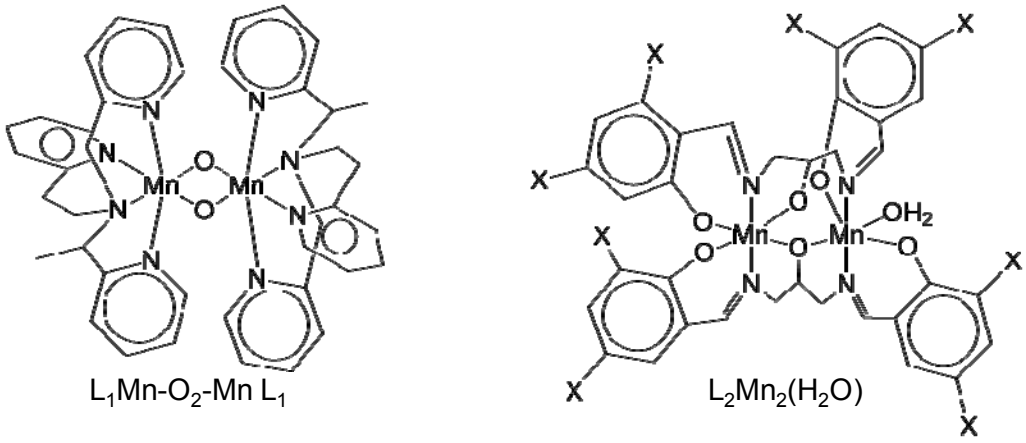

Scheme 1

Table 2 **One electron Redox Potentials for two Mn oxy bridged Dimers**

E^0 Reduction Potentials (V vs NHE)

Couple [a]	$L_1Mn\text{-}O_2\text{-}Mn\ L_1$ [b]	$L_2Mn_2(H_2O)$ [c]	$L_2Mn_2(H_2O)$ [c] → $L_2Mn_2(HO)$ [c]
$[III]_2/[III,IV]$	0.285	0.74 [d]	0.74 [d]
$[III,IV]/[IV_2]$	1.085	>1.6 [d]	0.95 [e]

a) From refs [36].

b) L_1 : (2-(2-pyridyl)ethyl)bis(2-pyridylmethyl)amine [36a].

c) L_2 : 2-hydroxy-1,3-bis(3,5-Cl_2-salicylideneamino)propane [36b].

d) No de-protonation this step, e) De-protonation this step.

Although the effect is not quite as dramatic as for the oxy-hydroxides, single proton loss from a terminal H_2O group maintains successive Mn single electron redox potentials within ~ 0.2V, while the absence of such compensation causes the second single electron potential to be nearly a volt higher than the first. Also, it is notable that the potentials for the L_2 complex, which has a N/O ligand ratio of 0.5, are substantially larger, all else being equal, than those for the L_1 complex, where the N/O ligation ratio is 2. Thus, consistent with the discussion of the previous section, predominant O ligation and the opportunity for charge compensation through proton loss from terminal hydroxy species, allows redox potentials to be maintained near 0.9 V, even for this (limited) system which is not particularly close, chemically, to the OEC Mn cluster. In total, the above observations speak closely to the existence of a broad, generic principle operating with oxo-Mn chemistry, which makes it uniquely suitable for the water oxidase site in PS II. The Mn ligand environment should be mainly oxygen-based to establish potentials near 0.9 V for oxidation states from II to IV, and terminal H_2O groups should (initially) be present to permit redox 'levelling' through progressive proton loss as the S states advance.

There is a further property of Mn, with parallel behaviour in Co, which is likely relevant to the utility of both metals in water oxidase catalysts generally. As we have seen, in their III and IV oxidation states, with predominantly O ligation, Mn and Co have redox potentials sufficient for 4 electron oxidation of water at neutral pH. XANES data show that the mean redox levels in the oxidized catalytic states are ~ +3.2 and ~ +3.7 for the Co phosphate and Mn birnessite catalysts, respectively [37,33e]. Redox potentials for Co in the II/III oxidation states are similar to those for Mn in the III/IV states (Table 1), so the two catalyst systems are close to equivalently poised when functioning. A further key similarity then exists between the Mn and Co systems, whose implications are currently under study by us. Both ions have a co-ordinatively stable configuration of the 3d orbitals in a higher oxidation state (d^3 for Mn^{IV} and low-spin d^6 for Co^{III}), but a Jahn-Teller destabilized configuration in the next lowest oxidation level (high-spin d^4 for Mn^{III} and low-spin d^7 for Co^{II}). This allows a possible reaction pathway, illustrated schematically for the Mn case in Fig. 5B. An initial *two-electron* oxidation of two adjacently ligated water/hydroxyl groups (the most difficult step) generates a peroxo group bound between two oxo-bridged metals in the higher oxidation state, with the electrons initially reducing other high-valent ions in the cluster. Internal electron transfer switches one of the peroxo bound metal ions to the lower, Jahn-Teller active oxidation state, which permits weakening of one metal-peroxo bond and then rapid final oxidation of the singly bound peroxo group to O_2. For Co, this may involve facile inter-conversion of Co^{II} between octahedral and tetrahedral coordination, a well known process in Co^{II} chemistry. Stranger

et al. have previously shown that these steps cannot occur in oxo-Mn *dimers*, a minimum *trimer* structure is necessary for this critical oxidation state transfer [38].

Mechanistic Implications for the Mn cluster in the OEC

From the above, water molecules are expected to play two key roles in the catalysed process of water oxidation. One obviously is to provide the substrate for the reaction, but the second, to provide the terminal ligand groups for redox levelling, is equally crucial. It is not obvious however whether these roles can be combined, the substrate species also providing the redox levelling through progressive proton loss, or whether distinct water molecules are separately employed for each function. In principle, both possibilities seem plausible, particularly for the inorganic catalysts (Fig. 5B).

Over the last decade, several groups have proposed detailed mechanisms for water oxidation in the OEC, which have evolved as structural resolution of the site has increasingly improved. A comprehensive review of earlier, qualitative models has been given by McEvoy and Brudvig [39], while later, computationally based mechanistic schemes are also reviewed in [23]. At present the most detailed models, which like our own studies also compute DFT derived structures for all the S states, have been given by Seigbahn [25] and Batista et al. [26]. Although the latter models are distinct (discussed in [23]) and appear to be undergoing continuous refinement, they and essentially all published models from groups other than the present authors share two key features:

i) At least one substrate water is ligated to Mn(4) and by S_3 this is fully *deprotonated* and present as a terminal or bridging (to Ca) oxo. Mn (4) has the IV oxidation state.
ii) In S_4 a bound oxy radical is generated by electron withdrawal and O-O bond formation is initiated by nucleophilic attack on this radical by a bridging oxy group or water bound to Ca.

Although the discussions may not usually have been framed in the terms employed here, these models, as a class, implicitly or otherwise suppose that the substrate waters participate, at least partially, in the redox levelling function.

Given the new molecular detail afforded by the 1.9 Å structure, it is instructive therefore to examine the OEC organization in light of the above considerations. In Fig. 4, four O groups, which are not bridges, are identified as being closest to the likely reactive portion of the cluster. Two (green box) are spatially close in a 'cleft' like region, involving Ca and Mn(1), Mn(3), and Mn(4), without being obviously fully ligated to any Mn. They are almost certainly waters, suggested by their bond lengths

to nearby metals (2.4-2.8 Å).‡ The second two (starred) are clearly ligated to Mn(4) alone, with bond lengths (~ 2.1 Å) which indicate that they would probably be waters in the lowest S state(s). This arrangement is suggestive of 'separate roles' for the respective water species, with those on Mn(4) being the redox levellers. That there are *two* such groups on Mn(4) and that these are the *only* likely candidates for leveller function, from the XRD structure, means that Mn(4) might progress through *two* redox steps (i.e. from II to IV) as the S cycle advances. From the data in Table 1 this is plausible, while maintaining a cluster oxidation potential near 0.9 V.

The kinetics of substrate water exchange with the OEC site during S state turnover provide a telling story here. Wyrzynski, Hillier et al. [17] have determined the exchange rates of substrate water with the OEC cluster in all S states. The results are summarised in Fig. 3. Basically, in all S states, two distinct exchange rates are seen, a 'fast' and 'slow' rate. The slow rate, which presumably corresponds to the more tightly bound substrate species and for which the data are best resolved, exhibits a counter-intuitive behaviour. It generally shows no monotonic change in the exchange kinetics as might be expected from a progression of H_2O, OH^- to O^{2-} substrate species, bound to Mn sites of ever increasing oxidation level. Rather, the resolved kinetics are quite similar in all S states except S_1, where the tighter bound water exchanges ~ 100 fold more slowly than in the other states, for which the rate is ~ seconds^{-1}. Further, Brudvig et al. have recently shown [40] from ^{17}O labelling experiments, that bridging oxo's in $Mn^{III,IV}$ catalase (and S_1 state PS II) exchange only on the hours time scale, making it unlikely that bridging O groups constitute the substrate species in the WOC. These data appear to us particularly constraining in total and point strongly towards a mechanism in which the substrate waters are quasi-terminally bound and distinct from the redox levelling waters throughout the S cycle (to S_3 at least).

We have shown computationally [24d] that this pattern of substrate water exchange is energetically consistent with the low oxidation state model and a cluster configuration in which substrate waters are located as in Fig. 4, with neither directly ligating Mn(4), unlike that proposed in all other mechanistic models [23]. The strongly bound water is ligated principally to Ca (Fig. 6) in our modelling (also in [26]) and this is consistent with the Ca/Sr replacement effect seen on the slow rate in substrate exchange kinetics [17c]. In S_1 this water actually becomes an hydroxide, through transfer of a proton to an oxo bridge joining Mn(3) and Mn(4), which reverses in S_2 ([24d] and Fig. 6). Our published and most recent studies (summarised, Fig. 6) suggest that the two oxy species on Mn(4) are both waters in S_0, but progressively deprotonate, so that by S_3 at least one and probably

‡ Our own calculations (Petrie et al. in preparation) indicate that if either water were in fact an OH^- group (e.g. as suggested in [5]), the O-metal (particularly Mn) distance(s) would be particularly shorter (~ 2.0 Å).

both have become hydroxides, with one of these now forming an additional (hydroxo) bridge to Mn(3). This structure is consistent with EXAFS studies [18,41], which detect a significant re-arrangement of the cluster in S_3. The latter structural change has been interpreted as formation of an additional short (~ 2.8 Å) Mn-Mn vector in S_3, slightly longer than the two ~ 2.7 Å vectors seen in S_1 and S_2 [18], or elongation of these two short Mn-Mn vectors to ~ 2.9 – 3.0 Å. [41]. Intriguingly, the computations at present suggest a picture which is a combination of these interpretations, with formation of an extra hydroxo bridge between Mn(3) and Mn(4) (shortening the Mn-Mn distance to ~ 2.9 Å) and some elongation of the previously short Mn(2)-Mn(3) distance (from 2.7 to ~ 2.9 Å)! The mechanistic significance of these results is presently under detailed study, particularly in regard to the 'suggestively' close location of the two substrate water molecules in S_3, both H bonded to the same oxo group bridging Mn(3) and Mn(4). This may indicate similarities of the water oxidase reaction to elements within the catalase substrate oxidative reaction (Fig. 1c).

Fig. 6 also indicates the Mn oxidation state sequence suggested by our modelling. Consistent with the discussion above on redox levelling, it is Mn(4) that contributes most to redox accumulation up to S_3, with Mn(1) and Mn(2) remaining invariant at the III level. Only Mn(2), which is 'ligand saturated' within the cluster and does not communicate directly with any exchangeable water/hydroxide group, undergoes oxidation (from III to IV) on the $S_0 \rightarrow S_1$ transition. Thus, the general 'insensitivity' of the substrate water binding to the increasing level of redox accumulation in the OEC cluster is readily understood. Further, proton loss in S_2 and S_3 is from the terminal water groups on Mn(4), adjacent to a likely proton exit channel commencing at Asp 61, which has been previously identified in the structure [42] . The putative proton channel also contains a Cl^- ion. This proposal is further supported by computational modelling suggesting Asp 61 as the natural 'proton exit' point within the cluster [43]. Interestingly, the formal cluster charge state is zero in S_1 and higher S states, but negative (-1) in S_0. Although no great significance should probably be accorded this, as the protein matrix is not included, it is notable that S_1, (not S_0) is the normal 'dark stable' state of the enzyme, i.e. the state of lowest total Mn oxidation level that is still net neutral.

In S_3 the cluster oxidation state configuration is III,IV,III,IV in this 'low oxidation state' picture. In principle, the transient S_4 state could involve a further Mn oxidation, but evidence from several sources suggests now that this is unlikely (see ref [23] for discussion). The S_4 state appears to be a 'compound event' with a sequence of steps [44], whose total duration (~ 50 –200μs) depends on the PS II preparation [45], involves ~ 1 proton release ($t_{1/2}$ ~ 30μs) [46] and exhibits no detectable change in mean Mn oxidation level from S_3 on the μs time scale [18b, 46]. It is likely that Y_z is oxidised throughout, as no detectable kinetic distinction occurs (at tens μs level) between O_2 release

and $Y_z^{\bullet}$ re-reduction [47]. At the beginning of the S_4 'sequence' the substrate is present as two water molecules, essentially as they existed in S_3. This suggests that the actual, concerted four electron O_2 forming reaction may be regarded formally as;

$$2H_2O + Mn(IV_2\,III_2)\,(S_3) + Y_z^{\bullet} \rightarrow O_2 + 4H^+\,(pH\sim6) + Mn(III_3\,II)(S_0) + Y_z \qquad 7)$$

Based the Mn data in Table 1 and the known potential for the $Y_z/Y_z^{\bullet}$ couple, the ΔG for this reaction is ~ -0.6 eV. This is modestly exothermic and subject of course to uncertainties regarding the equivalence or otherwise of the redox properties of hydrated Mn oxides to those of the OEC cluster components. However, it is certainly in the range of recent experimental estimates of the exothermicity of the reaction, from the insensitivity of O_2 release yield to oxygen back pressure during turnover, which suggest $\Delta G < -220$mV [48]. Thus, *prima facie*, there appears to be no *thermodynamic* need to invoke Mn oxidation levels higher than a mean value of 3.5 in S_3 to achieve water oxidation. Indeed even a value of ~ 3.0 would in principle suffice, from this standpoint, but would mean a value of ~ 2.0 in S_0, which would likely render the cluster structurally unstable. While the above conclusions are somewhat surprising from the standpoint of synthetic Mn complex chemistry, such as discussed in [2] for example, they are clearly within the realm of independent precedent for Mn, if *all* the special circumstances *known* to obtain within the OEC are applied - particularly the very low N/O ratio of the ligands. We should perhaps not be surprised if nature 'pulled out all the stops' and employed 'every trick in its bag' to achieve the remarkable efficiency of electrolytic water splitting that this enzyme centre, vital to nearly all life on earth, manages.

Thermodynamic possibility however, does not automatically ensure kinetic facility and the system must operate with a low (probably < 40 kJ/mol) activation barrier. In particular, extensive computational studies by Siegbahn and others [25,26] have shown that the only facile mechanism for O-O bond formation involves a formal $O^{\bullet}$ radical attack on a water or hydroxy species, which our own work to date broadly supports. This step is readily achievable in the above cited mechanistic models, because the substrate water(s) there undergo(es) progressive de-protonation during the S cycle (as proposed by them), or enter effectively as hydroxide at a late stage. In a picture more naturally consistent with the OEC substrate water exchange behaviour, where these waters are fully protonated up to and including S_3, 'finessing' the proton removal-exchange (e.g. onto the hydroxy groups on Mn(4) and the Mn-O-Mn bridge, Fig. 6 S_3) during the S_4 sequence, while retaining a sufficiently low reaction pathway energy profile , will be challenging. This is now the focus of our current computational studies and progress to date has been very encouraging.

Towards the Design of Bio-Mimetic Catalysts:

The ultimate aim of our work is to use our understanding of existing catalysts, particularly PS II, to design new catalytic components with activities approaching those of the natural system, but suitable for industrial scale electrolytic H_2 production. This will be challenging and directed by outcomes of our present investigations, yet unfinished. The particular directions employed here into understanding the organization and catalytic detail of the OEC are unique and will drive our computational exploration of the possibilities. One novel strategy based on our understanding of the OEC to date, is illustrated in Fig. 7. As outlined above, our computational work now strongly suggests that most redox accumulation actually occurs in Mn(4), outside the μ_3-oxo bridged sub-cluster (Fig. 7a). Thus Mn(4) acts as a 'battery' and therefore may be *catalytically* unnecessary. It might be replaced by another constant voltage electron sink (i.e. an electrode). Then a smaller metal cluster, such as that indicated schematically in Fig. 7c, could function as the water oxidase. This system involves an open edged cubane like our model of the OEC. Initially, computations will aim to establish:

i) The *minimum* nuclearity of the catalytic cluster, i.e. $(Mn)_3$, $(Mn)_3$/Ca, etc. As already noted, a Mn dimer is not suitable [38], but establishing function in a Mn trimer would have a huge synthetic advantage.

ii) The nature and connectivity of the bidentate bridges. These could be phosphinate groups (like the cubane catalyst of Dismukes et al. [49]) attached to covalently linked aromatic or aliphatic moieties. Links could be chemically equivalent (ab, a′b′) or in-equivalent (a′a, b′b) to enforce an open edged structure.

The system would operate at Mn redox levels equivalent to the OEC which is close to charge neutral. A functioning system could then be incorporated into a Nafion type polymer support, or some other immobilising substrate surface (e.g. [50]).

Acknowledgements

R.S. and R.J.P. gratefully acknowledge financial assistance from the Australian Research Council. The authors also acknowledge the generous provision of supercomputing time on the platforms of the NCI (National Computational Infrastructure) Facility in Canberra, Australia, which is supported by the Australian Commonwealth Government.

References

1 M. M. Najafpour, Govindjee, *Dalton Trans.,* 2011, **40**, 9076–9084

2 M. Wiechen, H.-M. Berends P. Kurz, *Dalton Trans.,* 2012, **41**, 21-31

3 R. E. Blankenship, H. Hartman, *Trends in Biochemical Sciences* 1998**, 23**: 94-97

4 R.J. Pace, 'An Integrated Artificial Photosynthesis Model' in 'Artificial Photosynthesis', A. Collings, C Critchley eds. Wiley-VCH, 2005, Chap. 2

5 Y. Umena, K. Kawakami, J.-R. Shen, N. Kamiya, *Nature* 2011**, 473,** 55-60

6 K. Satoh, T. Wydrzynski, Govindjee. Photosystem II: The Light Driven Water: Plastoquinone Oxidoreductase, Springer, Dordrecht, The Netherlands, 2005.

7 J. S. Vrettos, D. A. Stone, G. W. Brudvig, *Biochemistry* 2001**, 40,** 7937-7945

8 G. C. Dismukes, *Chem. Rev*. 1996**, 96**, 2909-2926

9 D.E. Wilcox, *Chem. Rev*. 1996**, 96**, 2435-2458

10 A. K. Holley, V. Bakthavatchalu, J. M. Velez-Roman, D. K. St Clair, *Int. J. Mol. Sci,* 2011**, 12**, 7114-7162

11 G. E Borgstahl, H. E. Parge, M.J. Hickey, W. F. Beyer Jr, R. A. Hallewell, J. A. Tainer , *Cell,* 1992**, 71**, 107–18

12 P. Chelikani, I. Fita , P. C. Loewen, , *CMLS, Cell Mol. Life Sci.* 2004**, 61**, 192-208

13 a) E. Jacobsen, *Acc. Chem. Res.* 2000 **,33**, 421-431, b) Y. Shimazaki, T. Nagano, H. Takesue, B.-H. Ye, F. Tani, and Y. Naruta, *Angew. Chem. Int. Ed.* 2004, **43**, 98 –100

14 V. V. Barynin, M. M. Whittaker, S. V. Antonyuk, V. S. Lamzin, P. M. Harrison, P. J. Artymiuk, J. W. Whittaker, *Structure*, 2011**, 9**, 725–738

15 D. Kuzek , R. J. Pace, *Biochimica et Biophysica Acta - Bioenergetics* 2001**, 1503**, 123-137

16 a) C. W. Hoganson, G. T. Babcock in: A. Sigel, H. Sigel (Eds.), Biological Processes in Metal Ions in Biological Systems, vol. 37, Marcel Dekker, New York, 1999**,** pp. 613-656, b) D. A. Cherepanov, W. Drevenstedt, L. L. Krishtalik, A. Y. Mulkidjanian, W. Junge, W. in G. Garab (Ed.) Photosynthesis: Mechanisms and Effects 1998 vol . **II,** 1073-1076,

17 a) W. Hillier, T. Wydrzynski, *Biochimica et Biophysica Acta - Bioenergetics,* 2001**, 1503**, 197-209 b) G. Hendry, T. Wydrzynski, *Biochemistry,* 2002**, 41**, 13328-13334 c) G. Hendry, T. Wydrzynski, *Biochemistry,* 2003**, 42**, 6209-6217

18 a) M. Haumann, C. Müller, P. Liebisch, L. Iuzzolino, J. Dittmer, M. Grabolle, T. Neisius, W. Meyer-Klaucke, H. Dau, *Biochemistry,* 2005**, 44**, 1894-1908 b) M. Haumann, P. Liebisch, C. Müller, M. Barra, M. Grabolle, H. Dau, *Science* 2005, **310**, 1019-1021

19 F. Rappaport, J. Lavergne, *Biochim. et Biophys. Acta,* 2001**, 1503**, 246-259

20 B. Loll, J. Kern, W. Saenger, A. Zouni, J. Biesiadka, *Nature,* 2005**, 438**, 1040-1044.

21 A. Guskov, J. Kern, A. Gabdulkhakov, M. Broser, A. Zouni, W. Saenger, *Nature Structural & Molecular Biology,* 2009**, 16**, 334-342.

22 S. Luber, I. Rivalta, Y. Umena, K. Kawakami, J.-R. Shen, N. Kamiya, G. W. Brudvig, V. S. Batista, *Biochemistry,* 2011**, 50**, 6308–6311

23 P. Gatt, R. Stranger, R. J. Pace, *Journal of Photochem. & Photobiol. B,* 2011**, 104**, 80–93

24 a) S. Petrie, R. Stranger, R. J. Pace, *Chem. Eur. J.,* 2007,**13**, 5082-5089 b) S. Petrie, R. Stranger, R. J. Pace, *Chem. Eur. J.,* 2008**, 14**, 5482-5494 c) S. Petrie, R. Stranger, R. J. Pace, *Angewandte Chemie-International Edition,* 2010 **, 49**, 4233-4236. d) S. Petrie, R. Stranger, R. J. Pace, *Chem. Eur. J.,* 2010**, 16**, 14026 – 14042.

25 P. E. M. Siegbahn, *Accounts of Chemical Research,* 2009**, 42**, 1871-1880.

26 E. M. Sproviero, J. A. Gascón, J. P. McEvoy, G. W. Brudvig, V. S. Batista, *J. Am. Chem. Soc.,* 2008**, 130**, 3428-3442.

27 J.-H. Su, N. Cox, W. Ames, D. A. Pantazis, L. Rapatskiy, T. Lohmiller, L. V. Kulik, P. Dorlet, A. W. Rutherford, F. Neese, A. Boussac, W. Lubitz, J. Messinger, *Biochimica et Biophysica Acta-Bioenergetics,* 2011, **1807** , 829-840

28 V. K. Yachandra, K. Sauer, M. P. Klein, *Chem. Rev*., 1996**, 96**, 2927-2950.

29 J. Dasgupta, G. M. Ananyev, G.C. Dismukes, *Co-ord. Chem. Rev*., 2008**, 252,** 347-360

30 a) A. R. Jaszewski, R. Stranger, R. J. Pace, *Phys. Chem. Chem. Phys.,* 2009**, 11**, 5634-5642. b) A. R. Jaszewski, R. Stranger, R. J. Pace, *Chem. Eur. J.,* 2011**, 17**, 5699 – 5713

31 K. Yamagouchi , D. T. Sawyer, *Inorg. Chem.,* 1985**, 24**, 971-976

32 S. Mukhopadhyay, S. K. Mandal, S. Bhaduri , W. H. Armstrong, *Chem. Rev.* 2004**, 104**, 3981□4026

33 a) M. Kanan, D. Nocera, *Science,* 2008**, 321**,1072-1075, b) Q. Yin, J. M. Tan, C. Besson, Y. V. Geletti, D. Musaev, A. E. Kuznetsov, Z. Luo, K. I. Hardcastle , C. L. Hill, *Science,* 2010**, 328**, 342–345 c) F. Jiao, H. Frei, *Angew. Chem. Int. Ed*. 2009, **48**,1841-1844, d) D. M. Robinson, Y. B. Go, M. Greenblatt and G. C. Dismukes (2010) *J. Am. Chem. Soc,*2010, **132**, 11467- 11469, e) R. K. Hocking, R. Brimblecombe, L.-Y. Chang[1,3], A. Singh[1], M. H. Cheah, C. Glover, W. H. Casey and L. Spiccia, *Nature Chem.,* 2011, **3**, 461-466

34 G. F. Swiegers, J. K. Clegg, R. Stranger, *Chem. Sci.,* 2011, **2**, 2254-2262

35 G. L. Elizarova, G.M. Zhidomirov, V.N. Parmon, *Catalysis Today,* 2000, **58**, 71–88

36 a) T. Aderemi, R. Oki, J. Glerup, D. J. Hodgson, *Inorg. Chem.,* **1990**, *29,* 2435-244, b) M. T. Caudle, V. L. Pecoraro *J. Am. Chem. Soc.,* 1997, **119**, 3415-3416

37 a) M. W. Kanan, J. Yano, Y. Surendranath, M. Dincă, V. K. Yachandra, D. G. Nocera, *J. Am. Chem. Soc.,* 2010,**132***,* 13692-13701, b) M. Risch, V. Khare, I. Zaharieva, L. Gerencser, P. Chernev, H. Dau, *J. Am. Chem. Soc.,*2009, **131**, 6936-6937

38 C. D. Delfs , R. Stranger, *Inorganic Chem.,* 2003, **42**, 2495-2503

39 J. P. McEvoy, G. W Brudvig, *Chem. Rev.*, 2006, **106**, 4455- 4483

40 I. L. McConnell, V. M. Grigoryants, C. P. Scholes, W. K. Myers, P. P.-Y. Chen, J. W. Whittaker, G W. Brudvig *J. Am. Chem. Soc.*, 2012 Just Accepted Manuscript, doi: 10.1021/ja203465y

41 W. Liang, T. A. Roelofs, R. M. Cinco, A. Rompel, M. J. Latimer, W. O. Yu, K. Sauer, M. P. Klein, V. K. Yachandra, *J. Am. Chem. Soc.* 2000, **122***,* 3399-3412

42 a) J. W. Murray, J. Barber, *J. Strut. Biol.* 2007, **159**, 228-237. b) H. Ishikita, W. Saenger, B. Loll, J. Biesiadka, E-W. Knapp, *Biochemistry* 2006, **45***,* 2063-2071. c) F. M. Ho, S. Styring, *Biochim. Biophys. Acta* 2008, **1777**, 140-153

43 A. R. Jaszewski, R. Stranger, R. J. Pace, *J. Phys. Chem. B,* 2011, **115**, 4484–4499

44 J. Buchta, M. Grabolle, H. Dau, *Biochimica et Biophysica Acta-Bioenergetics,* 2007, **1767** , 565-574.

45 M.R. Razeghifard, R.J. Pace, *Biochemistry,* 1999, **38** , 1252-1257.

46 F. Rappaport, M. Blanchard-Desce, J. Lavergne, *Biochimica et Biophysica Acta-Bioenergetics* 1994, **1184***,* 178-192.

47 a) M.R. Razeghifard, R.J. Pace, *Biochemistry* 1999, **38**, 1252-1257. b) M.R. Razeghifard, R.J. Pace, *Biochimica et Biophysica Acta-Bioenergetics* 1997, **1322**, 141-150

48 D. Shevela, K. Beckmann, J. Clausen, W. Junge, J. Messinger, *Proc. Natl. Acad. Sci. USA,* 2011, **108**, 3602–3607

49 G. C. Dismukes, R. Brimblecombe, G. A. N. Felton, R. S. Pryadun, J. E. Sheats, L. Spiccia, G. F. Swiegers, *Acc. Chem. Res.,* 2009, **42**, 1935– 1943

50 B. Cornell, G. Khrishna, P. Osman, R. Pace and L. Wieczorek, *Biochemical Soc. Trans.* 2001, **29**, 613-617

Figures

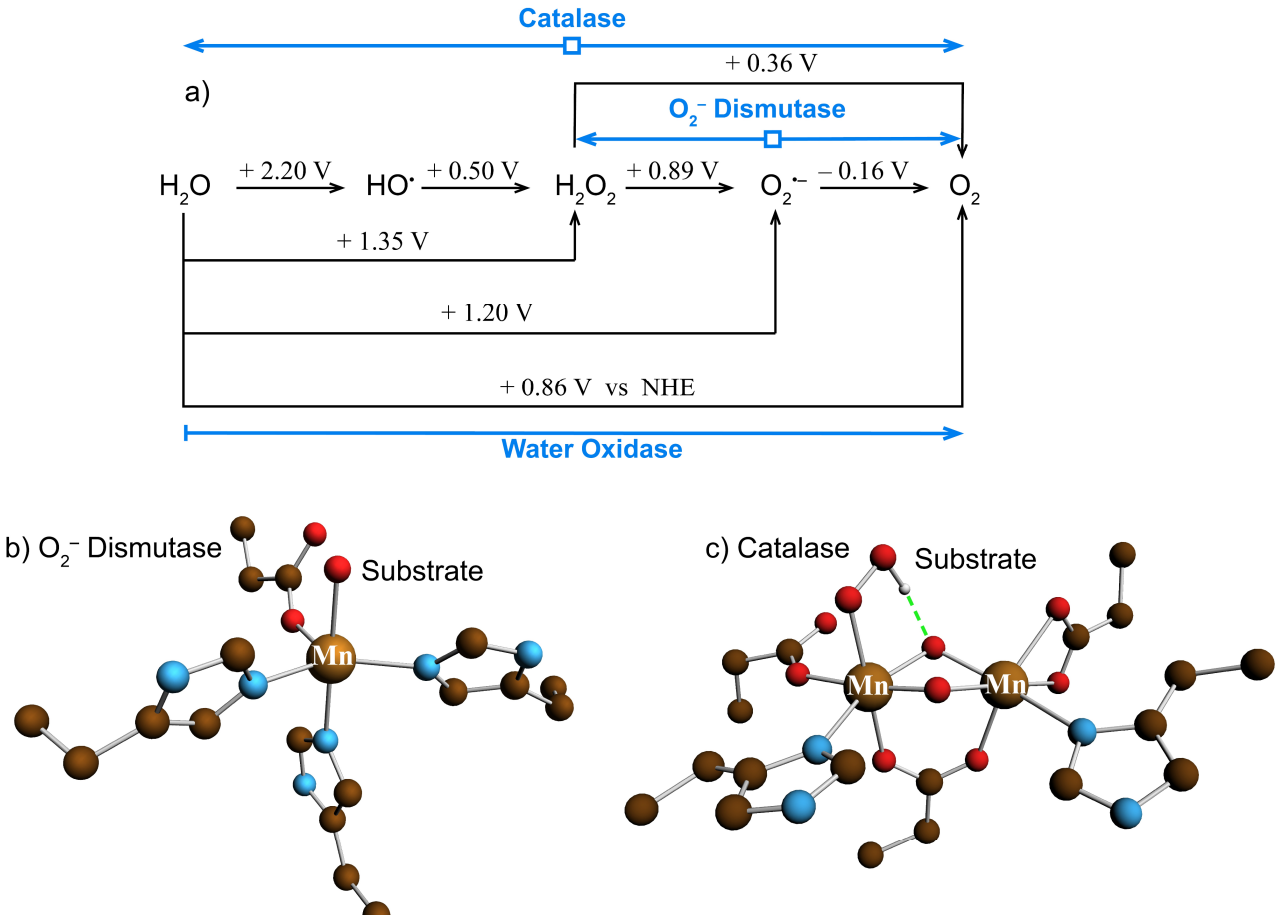

Fig 1
a) Redox potentials (as standard reduction potentials) at pH 7.0 and 298K for the oxidation of H_2O. Potentials are listed for oxidations ranging from one to four electron steps. Standard state of all species is unit activity (after Yamaguchi and Sawyer [31]). b) Local structure of the Mn catalytic site in Mn superoxide dismutase [11]. c) Local structure of the di-Mn catalytic site in Mn catalase, showing the proposed mode of peroxide binding during the substrate oxidative step (see text) [14].

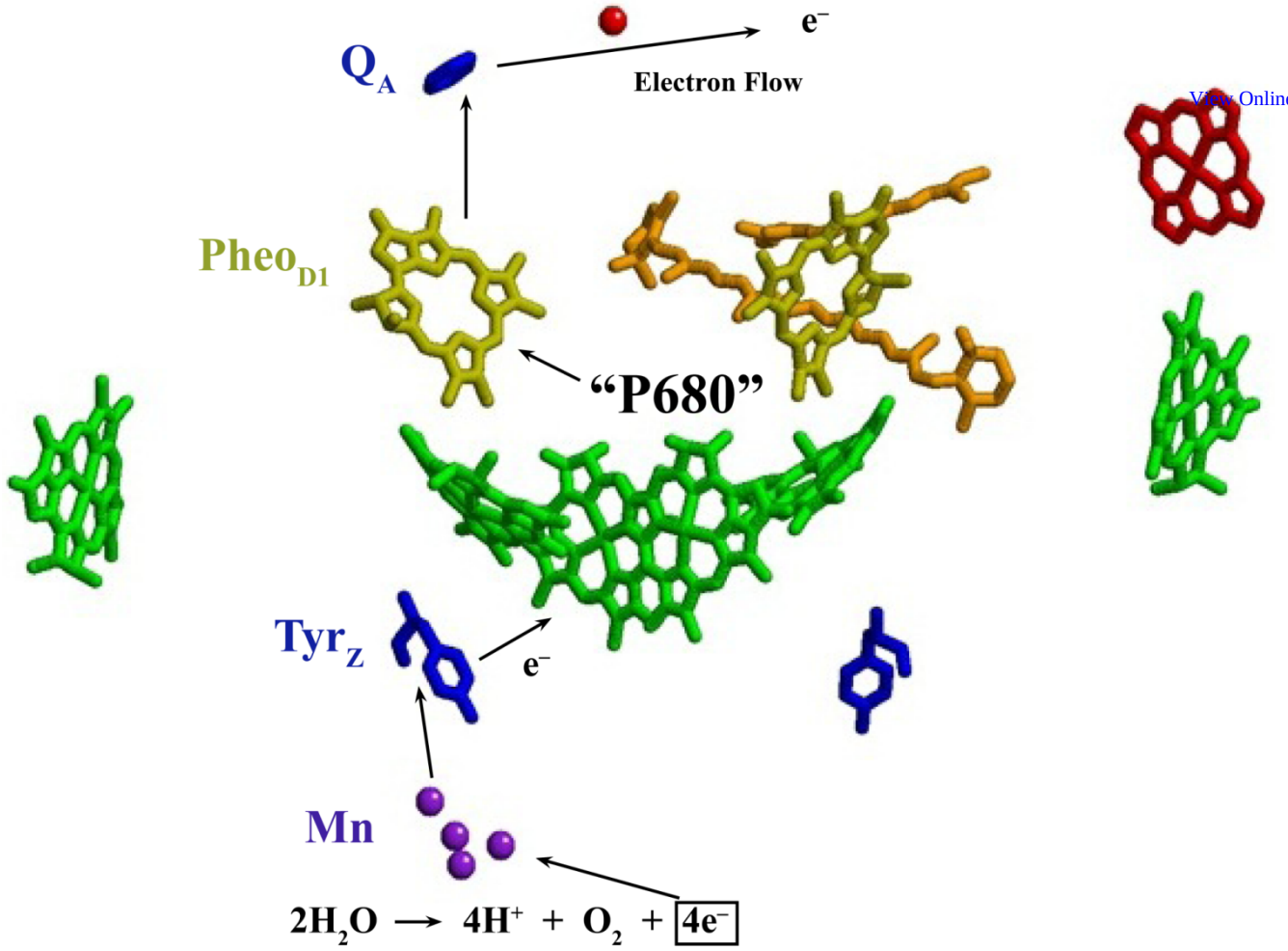

Fig 2
Structure of photosystem II complex near the reaction center region, with protein background removed (after [20]). Light energy is transferred from the chlorophyll antenna regions (CP 43, 47) to the P680 reaction centre special chlorophyll pair, which undergoes photo-oxidation. The released electron proceeds to the opposite membrane face and reduces, through Q_A and a non heme iron centre, a mobile plasto-quinone carrier, Q_B. The oxidised reaction centre is re-reduced by electrons, ultimately released from water, through an intermediate electron transfer species Y_z (tyrosine). This stabilises the charge-separated state against back reaction. The Mn_4/Ca cluster catalyses the water oxidation (4 electron process) and immobilises the reactive intermediates of this reaction.

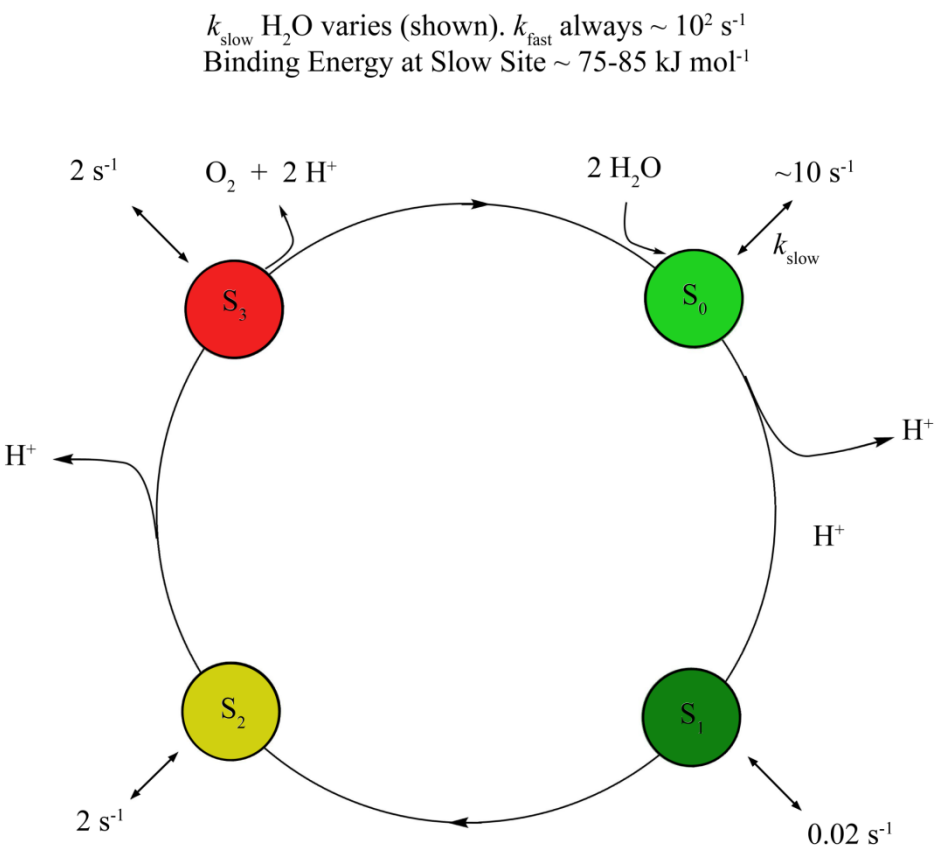

Fig 3
Schematic representation of S state cycle showing water exchange kinetics (from [17], using $H_2{}^{18}O$) and pattern of proton loss to external solvent [19] (idealised, see text). Two distinct rates of water exchange are seen, a 'fast' and 'slow' rate, corresponding to two substrate water molecules binding. The slow rate is well resolved in all S states and the fast rate resolved in S_2 and S_3, while it is unresolvably fast in S_1 and S_0. $^{36}O_2$ release measurements however are consistent with two substrate waters binding in all S states.

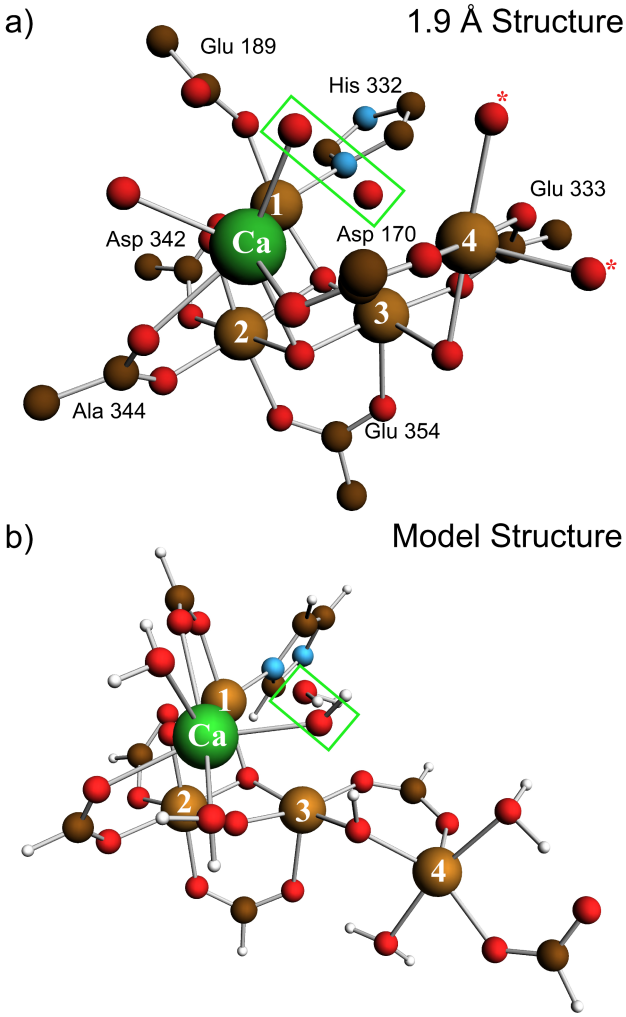

Fig 4
Comparison of the OEC region of the 1.9 Å structure of Umena et al. [5] (a) and our current computational modelling of a version of the S_1 state structure (b), proposed by us to be that most functionally relevant [24c, 24d]. Mn numbering as in [24]. The Mn oxidation states for Mn(1…4) are III,IV,III,II. Green boxed waters in 1.9 Å structure are proposed substrate species, while starred Oxy groups on Mn(4) are proposed terminal waters (in S_0) able to undergo deprotonation (see text). The most significant difference between the a) and b) structures is the location of Mn(4) relative to the Mn(1,2,3)Ca 'cube', which we have previously highlighted as the main source of structural variation that the cluster can execute. [24a]. This is also the region of greatest variation within the OEC as seen in the crystal structures [5,21]

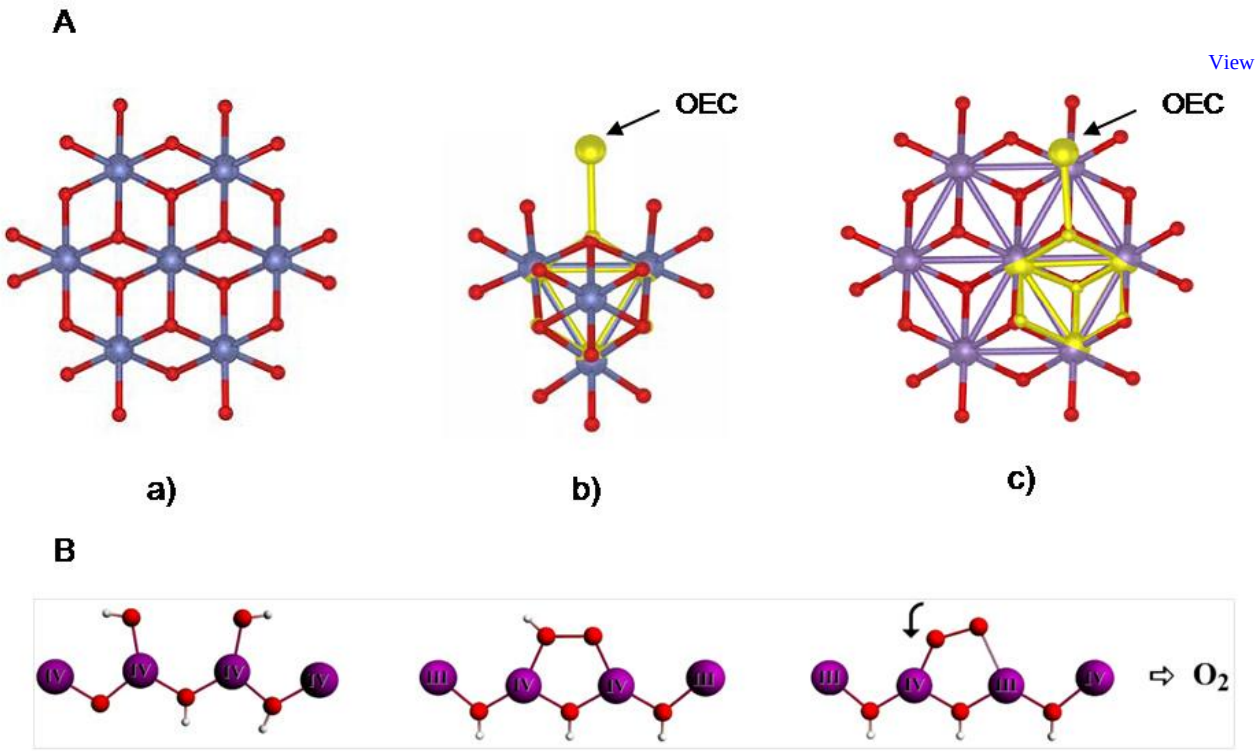

Fig. 5
A: Representative recent Water Oxidation catalysts: (a) Co-Phosphate edge-sharing molecular clusters of Nocera et al. [33a]. (b) B-site of Co_3O_4 spinel from nano-structured Co oxide on silica [33c]. (c) Surface of a Mn-O layer in K birnessite, (micro-clusters in nafion) [33e]. In all cases, metal (Co, Mn) ions are shown in blue and bridging oxygen atoms in red. Superimposed in (b) and (c) is an X-ray structure of the Mn-O core of the PSII-OEC shown in yellow (the Ca ion in the PSII-OEC has been excluded for clarity). Figs a)-c) from [34].
B: Possible reaction sequence for $2H_2O \rightarrow H_2O_2 \rightarrow O_2$, involving Jahn –Teller mobilization of Mn-O bond (see text)

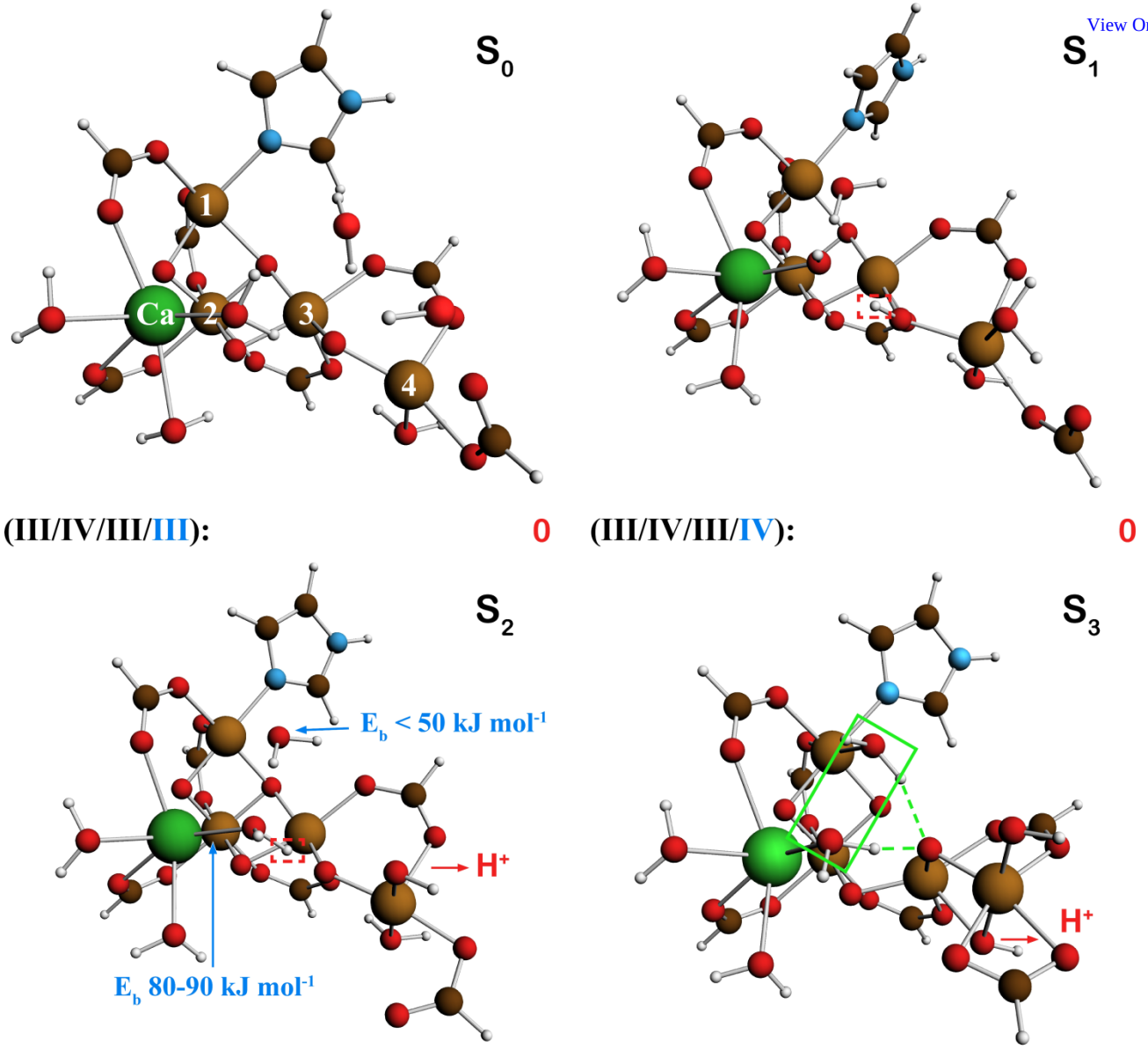

Fig 6
Computational structures of the OEC cluster in the four quasi-stable S states, $S_0..S_3$, according to our most recent proposals for the total charge and protonation levels in the site ([24c, 24d] and Petrie et al., in preparation). These are from our descriptions of the Type **II** structure, suggested as the 'active' geometry during functional turnover. De-protonation of terminal water on Mn(4) occurs on the $S_1 \rightarrow S_2$ and $S_2 \rightarrow S_3$ transitions, broadly consistent with the proton loss sequence in Fig. 3, if internal release from the cluster is partially uncoupled from release to the solvent (see text). Recent calculations [Petrie et al. in preparation] suggest that the second deprotonation in S_3 triggers formation of an extra hydroxo-bridge between Mn(3) and Mn(4), as inferred from EXAFS (see text) and shown. This positions substrate waters as indicated (green box). Shown are the Mn oxidation levels in the OEC (Roman numerals for Mn 1…4) and typical binding energies (E_b) for the substrate water molecules ('fast', $E_b < 50$ and 'slow' $E_b \sim 80$ kJ/mol) [24d] . The transferred proton in S_1, responsible for the very slow substrate exchange in S_1 is indicated (red square). Red figures denote total cluster charge. Computational methodologies as in [24]

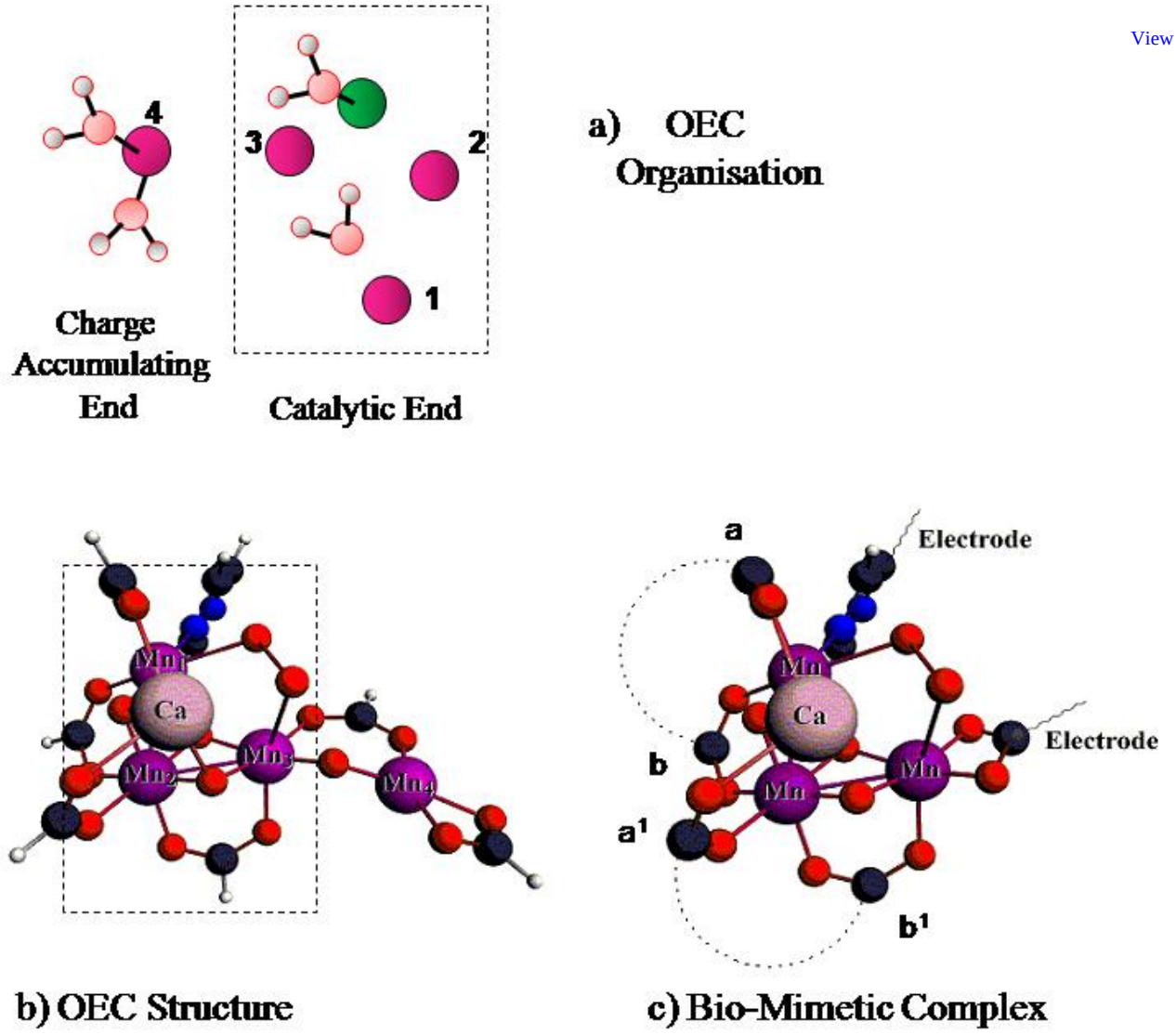

Fig 7
a) Diagrammatic location of the two 'water populations' in the OEC structure proposed here, defining the catalytic and charge accumulating regions. b) Schematic OEC structure (from Fig. 6, catalytic region boxed), showing location of possible O-O bond formation site. c) Possible Bio-mimetic water oxidase construct based on the molecular form of the OEC. The 'charge accumulating' function is now provided by an electrode surface.